



Removal of Neutral Red from aqueous solution using *Pleurotus ostreatus* nanoparticles by response surface methodology

Dai-Yin Lei, Bo Li, Qiao Wang, Bo Wu, Lan Ma, Heng Xu*

Key Laboratory of Bio-resources and Eco-environment (Ministry of Education), College of Life Science, Sichuan University, Sichuan, Chengdu 610064, China, Tel. +86 28 85414644, +02885414644; Fax: +86 28 85418262; email: xuheng64@sina.com

Received 28 July 2013; Accepted 6 March 2014

ABSTRACT

An adsorbent, *Pleurotus ostreatus* nanoparticles (PONS), was tested to remove the cationic dye Neutral Red (NR) from aqueous solution. Prepared PONS were characterized by scanning electron microscope (SEM) and Fourier transform infrared (FTIR) spectrometer. FTIR indicated the active groups involved in the adsorption. Main effect factors of adsorption were selected by Min Run Res V design. Then Box–Behnken design was applied to evaluate the interactive effects of the three most important variables. The experimental data were well fitted to Langmuir isotherm model and pseudo-second-order kinetic model. The maximum adsorption capacity of NR was 57.14, 59.17, and 61.73 mg g⁻¹ at 293, 303, and 313 K, respectively. The adsorption was spontaneous according to thermodynamics data. The results confirmed that PONS had the ability to be applied as an adsorbent for the removal of cationic dye from wastewater.

Keywords: *Pleurotus ostreatus* nanoparticles; Response surface methodology; Neutral Red; Adsorption

1. Introduction

Dyes are widely used in many industries such as textiles, paper, plastics, leather, and food to color products due to their stability to light, heat, and oxidizing agents [1,2]. In recent years, nearly 30 million tons of dyes have been produced in the world which exerts pressure on the environment directly or indirectly [3]. What is more, the emission of color from wastewater into environment brings pollution and great damage to human beings for its toxicity, mutagenicity, and carcinogenicity [4,5]. Because even a small quantity of dye in water can be toxic and highly visible, removal of dyes and pigments from waste efflu-

ents becomes environmentally important [6]. A number of methods which remove dyes from textile effluents have emerged such as chemical coagulation, flotation, chemical oxidation, filtration, membrane separation, ion-exchange, aerobic, and anaerobic microbial degradation [7]. However, adsorption is supposed to be the most popular physicochemical treatment for the removal of dissolved organics from water [8].

Currently, a large number of researches on the adsorption of dyes from solutions by adsorbents such as spent mushroom [9], wheat straw [10], MCM-41 [11], mansonia wood sawdust [12], activated carbon [8,13], and citrus limetta peel [14] have been studied. Many of them studied the adsorption of dyes on micron level (150–1,000 μm) [15]. Due to their new and high adsorption abilities, nanoscale particles such as

*Corresponding author.

halloysite nanotubes [16] and alginate-halloysite nanotube beads [17] have drawn great attention of researchers recently.

Because of their biodegradable and nontoxic nature, and bind groups, biological resources are considered to remove dye ions from aqueous solution [18]. And amino, carboxyl, thiol, and phosphate groups existing in the fungal cell wall are responsible for binding dye molecule [19]. China as the largest edible fungi producer, consumer, and exporter in the world produces about 29 million tons of waste substrates excluding the edible fungi production every year, but most of them were abandoned [18]. These abandoned resources have economic and ecological potential values and can be reprocessed as bio-adsorbents to deal with dye wastewater. A survey of the latest literature shows that much work has been performed on species of fungal for the removal of different dyes from wastewater [20]. *Pleurotus ostreatus* belonging to white rot fungus is one of the widely cultivated mushroom species in China, and its production has increased over 500% in the last 10 years, ranking the second or the third position in the context of edible mushroom industrial production in the world. Furthermore, *P. ostreatus* substrates have been demonstrated to have the ability to discolor dye effluent [21].

As one of the cationic dyes, Neutral Red (NR toluylene red chloride, $C_{15}H_{16}N_4 \cdot HCl$, C.I. 50040, formula weight 288.78) was selected as the adsorbate in this study. *P. ostreatus* waste body was dried and then smashed into nanoparticles (PONS). The aim of the study was to evaluate the adsorption potential of PONS for NR removal. Up to now, no similar reports about this nanosize material were studied in dye removal.

2. Materials and methods

2.1. Chemicals

All reagents used in this study were of analytical grade purchased from KeLong (Chengdu, China). A stock solution ($1,000 \text{ mg L}^{-1}$) was prepared by dissolving NR in deionized water and the required concentrations were obtained when needed by diluting the stock solution with deionized water. Before mixing with adsorbents, the pH values were adjusted to desired values by HNO_3 (0.1, 1 M) or NaOH (0.1, 1 M), and the pH value was measured by a pH meter (Model PHS-25, calibrated with buffers of pH 4.00, 6.86, and 9.18).

2.2. Preparation of the PONS

Fresh *P. ostreatus* was obtained from a mushroom production site located in the suburbs of Chengdu,

China. It was washed thoroughly with deionized water, then oven dried at 323 K for 3 d, ground with a pulverizing mill (Joyoung, JYLC012) to obtain raw biomass. Then the raw powder was processed by the HENIG (Taijihuan, CJM-SY-A) drying 2 h at 373 K and continuous milling for 10 h. When the small particles reached up to a certain extent, they will lead to oxidation which was caused by increased surface areas, and then the phenomena of explosion will emerge. Therefore, nitrogen was added to reaction vessels to prevent oxidation, spontaneous combustion, and other adverse phenomena. At last, the prepared PONS were collected to further use.

2.3. Characterization of PONS

The surface morphology features of PONS were identified by scanning electron microscopy (SEM) (JSM-5900LV, Japan). The PONS powder was dispersed using ultrasonic disperser. Next, the sample was coated with gold for electron reflection and then was vacuumed for 5–10 min before analysis. The infrared spectroscopy analysis of PONS was obtained by using a Fourier transform infrared (FTIR) spectrometer (NEXUS-650, America). The spectra were recorded from $4,000$ to 400 cm^{-1} .

The pH at the point of zero charge (pH_{PZC}) of the PONS, namely the pH value required to give zero net surface charge, was determined by mass titration [22,23]. Three solutions with different initial pH values (3, 6 and 11, respectively) were prepared with the addition of 0.05 M aqueous solution of HNO_3 or NaOH, and $NaNO_3$ was used as the background electrolyte. For each initial pH, six Erlenmeyer flasks were filled with 30 mL of the solution and different amounts of PONS were added (0.05, 0.1, 0.5, 1, 5, and 10% by weight). Then the mixture was shaken for 24 h at a thermostatic swing shaker. The pH was measured after the PONS were separated. A plot of the equilibrium pH versus mass fraction yielded a curve showing a plateau and the pH_{PZC} was identified as the point at which the change of pH is zero. The pH_{PZC} was then taken as the average of the three asymptotic pH values.

2.4. Design of experiment

In this study, the experimental design methodologies were described in detail as follows. Design-Expert 7.0.0 (Stat-Ease, USA), which including Factorial Design, Response Surface Design, Mixture Design, and Combined Design, was used for experimental design and data analysis.

2.4.1. Min Run Res V design

Min Run Res V design is one of the Factorial Design. It is usually used to select important variables and has successfully been applied by researchers [24]. Min Run Res V design, a standard two-level factorial design, allows for estimation of main effects. It is an excellent design to reduce the number of runs and still obtain clean results.

Thus, Min Run Res V design was used in this paper to evaluate the factors that affected the uptake of NR. Six independent variables (pH, agitation speed, initial concentration, biomass loading, temperatures, and contact time) were taken to obtain removal rate (%) of the NR by biosorption onto PONS. The experimental design matrix is shown in Table 1.

2.4.2. Box–Behnken design

The response surface methodology (RSM) has its own properties and characteristics [25]. Central composite design, Box–Behnken design (BBD), and three-level factorial design are the most popular RSM designs applied by the researchers. BBDs are response

surface designs, specially made to require only three levels, coded as -1 , 0 , and $+1$. BBDs are available for 3–21 factors. They are formed by combining two-level factorial designs with incomplete block designs. Most importantly, this procedure creates designs with desirable statistical properties with only a fraction of the experiments required for a three-level factorial. Because there are only three levels, the quadratic model is appropriate. Furthermore, the BBD offers calculations of the response function at intermediate levels; owing to the careful design and analysis of experiments, it is possible to guess the system performance at any experimental point in the range [26–28].

Thus, RSM based on BBD was applied to evaluate interactive effects for NR removal. The three main factors, pH, initial concentration, and temperature were chosen by Min Run Res V design to be independent variables, and removal rate was considered as the response.

2.5. Batch experiments

Each experiment was carried out in 150 mL Erlenmeyer flask containing 50 mL NR solution; Erlenmeyer

Table 1
Experimental design matrix and responses of the Minimum Run Res V Design

Runs	Factors						Responses (% removal)
	pH	Agitation speed (rpm)	Initial concentration (mg L ⁻¹)	Biomass loading (mg L ⁻¹)	Temperature (°C)	Contact time (min)	
1	2	200	10	6	40	10	26.50
2	7	200	100	1	20	240	85.14
3	2	50	10	1	40	10	20.10
4	2	200	10	6	20	240	66.11
5	7	50	10	6	40	10	46.36
6	7	200	10	6	40	240	50.00
7	7	200	10	1	20	10	62.49
8	2	200	10	1	40	240	20.30
9	7	50	100	6	40	240	91.85
10	2	50	10	6	20	10	50.05
11	7	200	100	6	20	10	75.88
12	7	200	100	1	20	10	82.47
13	7	50	10	1	40	240	68.02
14	2	50	100	6	40	10	74.29
15	7	50	100	1	20	10	93.51
16	7	50	10	6	20	240	69.86
17	2	50	10	1	20	240	56.80
18	2	200	100	1	20	10	35.80
19	2	200	100	6	40	240	59.01
20	7	200	100	1	40	10	82.25
21	2	50	100	1	40	240	41.50
22	2	50	100	6	20	240	75.88

flask was shaken in a constant temperature breeding shaker (SUKUN, SKY-211B). The experimental factors of adsorption were adjusted according to experimental design. After adsorption, the solution was centrifuged for 10 min at 3,000 rpm and the concentration of residual NR was tested by UV/vis spectrophotometer at λ_{\max} of 530 nm.

2.5.1. Kinetics

About 1 g L^{-1} of PONS was shaken with initial concentration (50, 100, 150, 200 mg L^{-1}) of NR solution (pH 5) at 100 rpm and 293 K. Samples were taken at different time intervals from 5 to 300 min.

2.5.2. Isotherms

About 1 g L^{-1} of PONS was added in seven different initial concentrations ($10\text{--}200 \text{ mg L}^{-1}$) of NR solution (pH 5). Then the Erlenmeyer flask was shaken for 5 h at 100 rpm and 293, 303, and 313 K, respectively.

The NR removal percentage (R , %) was calculated according to the Eq. (1), adsorption amount at different time (Q_t , mg g^{-1}) was calculated according to the Eq. (2), and adsorption capacity (Q_e , mg g^{-1}) was calculated according to the Eq. (3):

$$R = \frac{100(C_0 - C_e)}{C_0} \quad (1)$$

$$Q_t = \frac{(C_0 - C_t)V}{M} \quad (2)$$

$$Q_e = \frac{(C_0 - C_e)V}{M} \quad (3)$$

where C_0 , C_t , and C_e (mg L^{-1}) are the initial, t time, and equilibrium concentrations of dye, respectively; V is the volume of solution (L); M is the adsorbent dose (g).

All the design experiments were carried out with three replications, and the result was showed by calculation of average. For each experiment, a blank with no adsorbent in 50 mL NR solution was shaken simultaneously to check out if there were any adsorption on conical flask wall.

3. Results and discussion

3.1. Characterization of the PONS

The SEM image of PONS is shown in Fig. 1. PONS were roughly sphere and had unsmooth surface. The average diameter of PONS was under 300 nm

indicating that the relatively large specific surface area might give them plenty of adsorption sites.

Fig. 2 shows the FTIR spectra of PONS before (a) and after (b) NR uptake. The previous researches have reported that almost all of the fungal materials exist in intense absorption bands around $3,500\text{--}3,200 \text{ cm}^{-1}$, which represent the stretching vibrations of amino groups. These bands were superimposed onto the side of the hydroxyl group band at $3,500\text{--}3,300 \text{ cm}^{-1}$ [29]. A similar and very strong peak was detected at about $3,450 \text{ cm}^{-1}$. The relatively weak peak at about $2,920 \text{ cm}^{-1}$ showed the characteristic stretching vibrations of the methyl and methylene (CH_n) groups [18]. The strong peak at around $1,650 \text{ cm}^{-1}$ was caused by the C=O stretching band of carbonyl groups. The phosphate groups showed some characteristic adsorption peaks around $1,150$ and $1,078 \text{ cm}^{-1}$ representing P=O and P-OH stretching, respectively. The deformation vibration between 610 and 535 cm^{-1} for the fungal preparation represents C=N=C scissoring and it is only found in protein structure [29]. The changes of these absorption peaks suggested the presence of responsible functional groups such as -NH, -OH, C=O, P=O, P-OH, and C=N=C in the PONS.

The pH_{PZC} of PONS was 6.16. When the pH was below the pH_{PZC} , the PONS surface was charged positively to limit the adsorption of NR. But, when the pH was above the pH_{PZC} of PONS, the surface was charged negatively to improve the adsorption of NR.

3.2. Screen of main factors by Min Run Res V design

Experimental design matrix and responses of the Minimum Run Res V Design are shown in Table 1. The removal rate (%) from 20.10 to 93.51 suggested

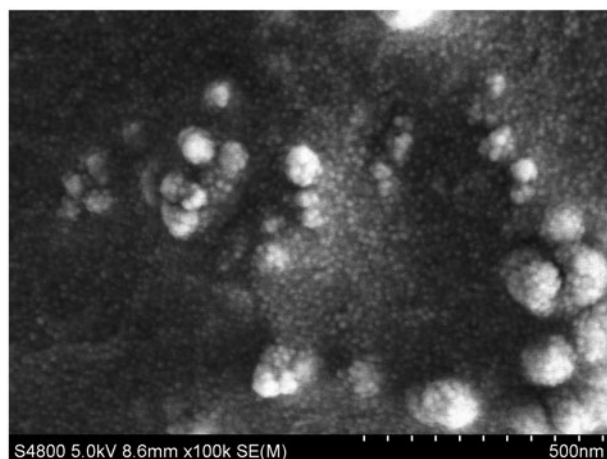


Fig. 1. TEM image of PONS.

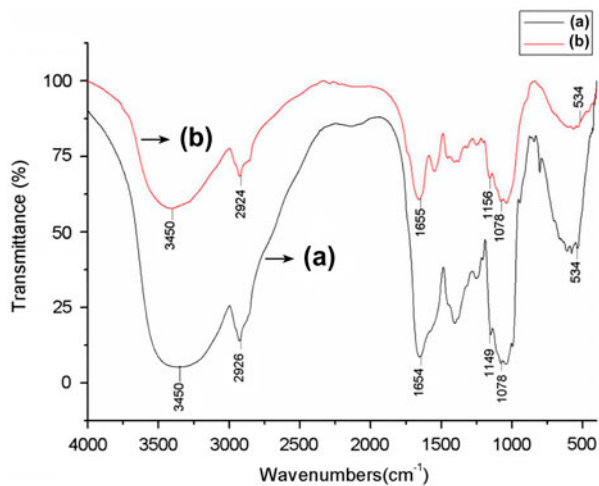


Fig. 2. FT-IR spectrum of PONS.

that the NR removal rate was ranged widely at different conditions. The analysis of variance (ANOVA) was applied to test the availability of Minimum Run Res V Design and the results are shown in Table 2. Values of “Prob > F” was less than 0.05 indicating that model terms were significant. The “Pred R-squared” of 0.5120 was in a reasonable agreement with the “Adj R-squared” of 0.6840. “Adeq Precision” measured the signal to noise ratio. A ratio greater than 4 was desirable. The ratio of 8.864 indicated an adequate signal. This model could be used to navigate the design space. NR removal is expressed as Eq. (4):

$$\text{Removal (\%)} = +60.64 + 12.19A - 3.99B - 11.17C + 3.75D - 6.81E + 3.62F \quad (4)$$

where *A* stands for pH, *B* stands for agitation speed, *C* stands for initial concentration, *D* stands for biomass loading, *E* stands for temperature, *F* stands for contact time.

Table 2
ANOVA of NR removal for variables fitted to Min Run Res V Design

Source	Sum of squares	df	Mean square	F-value	P-value	Prob > F
Model	7965.97	6	1327.66	8.58	0.0004	Significant
A	3172.00	1	3172.00	20.49	0.0004	
B	340.35	1	340.35	2.20	0.1589	
C	2661.14	1	2661.14	17.19	0.0009	
D	300.20	1	300.20	1.94	0.1841	
E	989.28	1	989.28	6.39	0.0232	
F	279.44	1	279.44	1.80	0.1991	
Residual	2322.37	15	154.82			
Cor total	10288.34	21				

Notes: $R^2 = 0.7743$; $R_{\text{Adj}}^2 = 0.6840$; $R_{\text{Pred}}^2 = 0.5120$.

The main effects plot of NR removal is shown in Fig. 3. Initial concentration, pH, biomass loading, and contact time had a positive effect. However, agitation speed and temperature had negative effects. The slopes of pH, initial concentration, and temperature were greater than others, indicating that pH, initial concentration, and temperature had significant effects on NR removal.

Therefore, the three significant factors were further studied by BBD, agitation speed for 100 rpm, biomass loading for 1 g L^{-1} , and contact time for 240 min in following experiments.

3.3. Analysis of BBD

The BBD matrixes of the experiments and the results are shown in Table 3. According to the fit summary of the software Design Expert, the quadratic model was suggested and selected. The final equation in terms of coded factors was expressed as Eq. (5):

$$\begin{aligned} \text{Removal (\%)} = & +85.95 - 1.18A + 17.82B + 0.61C \\ & - 2.75AB + 2.80AC - 1.90BC - 2.95A^2 \\ & + 13.20B^2 + 2.48C^2 \end{aligned} \quad (5)$$

where *A*, *B*, and *C* are defined in Table 3.

In order to ensure a good model, the ANOVA was applied and the results are shown in Table 4. The Model *F*-value (333.02) indicates that the model was significant. Values of “Prob > F” (<0.0001) indicating model terms were significant. The “Lack of Fit *F*-value” (0.19) implied the Lack of Fit was not significant compared to the pure, and the quadratic model was valid for the study [30]. The value of R^2 0.9977 and adjusted R^2 0.9921 were close to 1.0, which

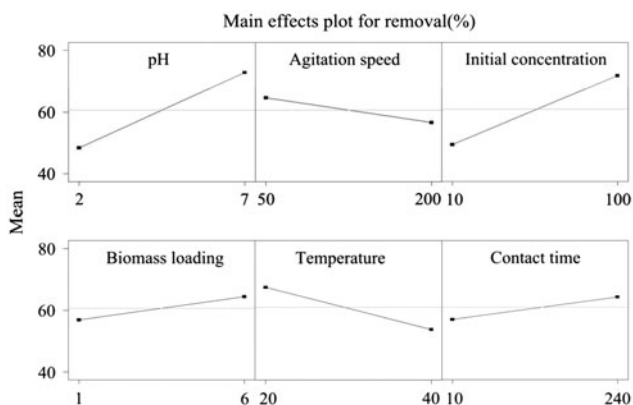


Fig. 3. Main effects plot for removal of NR by PONS.

indicated a high correlation between the observed values and the predicted values. This illustrated that the quadratic model provided an excellent explanation of the relationship between the independent variables and the responses [31].

The “Pred R -squared” of 0.9921 was in a reasonable agreement with the “Adj R -squared” of 0.9947. “Adeq Precision” measured the signal to noise ratio. A ratio greater than four was desirable. And the ratio of 53.525 indicated an adequate signal. This model could be used to navigate the design space.

3.4. Interactive effect of independent variables on NR removal

In order to study the interaction of the three factors, the three-dimensional (3D) response surface plots

based on the feasible quadratic model were constructed. 3D response surface plots provided a function of two independent variables which can vary within their experimental ranges. Furthermore, 3D response surface plots can maintain all other variables at fixed (center) levels, provide information on their relationships, and can be helpful in understanding both the main and the interaction effects of these two independent variables [32]. The quadratic model had three factors in this study; each plot set one of the variables constant at its center level to construct a total of three 3D response plots.

The response surface of initial NR concentration and pH value is shown in Fig. 4. The experiments were carried out at different initial concentration from 10 to 100 mg L⁻¹ and different pH from 3 to 7 at 303 K. The figure clearly pointed out that the NR removal rate was increased with the initial concentration from 10 to 100 mg L⁻¹; while the initial concentration was greater than 77.5 mg L⁻¹, the incremental removal rate became very slow. At the lower concentration, the PONS might gather by the -NH, -OH groups which lead to low removal rate. At the higher concentration, the dye cations could compete with the active sites of PONS and augment molecular collision with PONS. As a result, it increased the removal rate. When the pH was from 3 to 5, there was a slight rise of NR removal; while the pH was from 5 to 7, the remove rate was almost constant. The removal rate influenced by pH from 5 to 7 was similar to the spent cottonseed hull substrate [18]. Furthermore, the pH_{PZC} of PONS was 6.16, when the pH was from 3 to 5; under the

Table 3
BBD experiments and experimental results

Runs	A-pH	B-Initial concentration (mg L ⁻¹)	C-Temperature (°C)	Responses (% removal)
1	5	10	20	55.30
2	3	100	30	91.59
3	7	55	20	80.52
4	5	55	30	85.35
5	5	55	30	86.25
6	7	100	30	84.13
7	3	10	30	49.96
8	5	55	30	86.45
9	5	100	40	91.34
10	5	10	40	60.00
11	5	100	20	94.24
12	5	55	30	87.61
13	7	10	30	53.51
14	3	55	40	84.83
15	7	55	40	87.67
16	3	55	20	88.89
17	5	55	30	84.07

Table 4
ANOVA of NR removal for variables fitted to Box–Behnken model

Source	Sum of squares	df	Mean square	F-value	P-value	Prob > F
Model	3430.14	9	381.13	333.02	<0.0001	Significant
A-pH	11.14	1	11.14	9.73	0.0168	
B-Initial concentration	2539.35	1	2539.35	2218.85	<0.0001	
C-Temperature	2.99	1	2.99	2.61	0.1501	
AB	30.31	1	30.31	26.48	0.0013	
AC	31.42	1	31.42	27.45	0.0012	
BC	14.44	1	14.44	12.62	0.0093	
A ²	36.53	1	36.53	31.92	0.0008	
B ²	733.98	1	733.98	641.34	<0.0001	
C ²	25.83	1	25.83	22.57	0.0021	
Residual	8.01	7	1.14			
Lack of fit	1.02	3	0.34	0.19	0.8949	Not significant
Pure error	6.99	4	1.75			
Cor total	3438.15	16				

Notes: $R^2 = 0.9977$; $R_{Adj}^2 = 0.9947$; $R_{Pred}^2 = 0.9921$; Adeq Precision = 53.525.

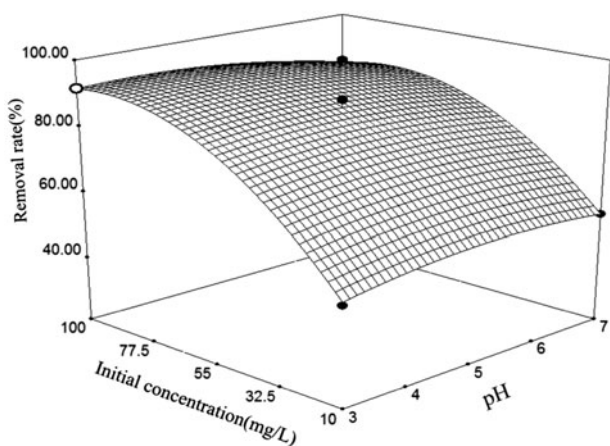


Fig. 4. The effects of initial concentration and pH on NR removal.

pH_{PZC} , the PONS surface was charged positively to limit the adsorption of NR. As NR is a cationic dye, it exists in aqueous solution in the form of a positively charged ion. And the PONS surface was negatively charged when the pH was above the pH_{PZC} . While the pH value was above 5, the removal rate did not rise as expected. At this point, the concentration of NR might be the main factor affected the removal rate compared to pH. The pH dependence of dye adsorption was mainly influenced by two factors: firstly, distribution of dye in the solution phase and secondly, overall charge of the adsorbent [16].

In the present paper, removal rate increased with increasing pH that could be attributed to electrostatic attraction of positively charged NR and negatively

charged surface of PONS. PONS contained significant amount of functional groups such as $-NH$, $-OH$ which was evidenced by FT-IR spectrum. At a lower pH, the surface of the PONS would be surrounded by the excess hydronium ions, which competed with NR cations. However at a higher pH, the surface of PONS may become negatively charged, which enhanced the adsorption of the dye cations through electrostatic attraction [18]. In total, both initial concentration and pH had positive effect on NR removal which was similar to the results of main effects plot.

Fig. 5 shows interactive influence of temperature and pH on NR removal of the PONS. The data were obtained at different pH values, which were from 3 to 7, and temperatures, which were from 293 to 313 K. The NR concentration was 55 mg L^{-1} . This figure clearly showed that at any fixed temperature, the remove rate increased with the increase of pH value; then it remained almost constant. The tendency was same as that in Fig. 4. The elimination capacity showed slight increase from 293 to 313 K at any particular pH. Generally, adsorption was an exothermic process; it would be expected that the increase of temperature would lead to decrease of removal rate. However, if the adsorption process was controlled by the diffusion process, the removal efficiency would show an increase with an increase in temperatures. This was basically due to the fact that the diffusion process was an endothermic process [33].

Fig. 6 shows the interactive of initial NR concentration and temperature on NR removal at pH 5. As shown in Fig. 6, the effect tendency of each factor is same as in the Figs. 4 and 5. At any fixed concentration, the removal rate increased from 293 to 313 K. In

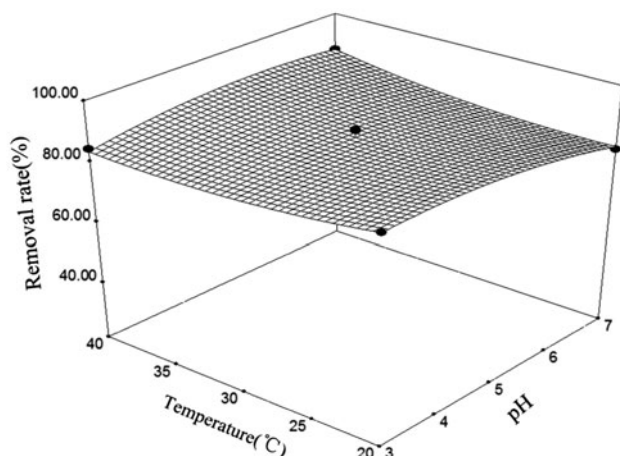


Fig. 5. The effects of temperature and pH on NR removal.

contrast, the removal rate increased with the increment of NR concentration at any temperature between 293 and 313 K.

In short, the maximum NR removal of 96.14% was obtained at pH 5.45, initial NR concentration = 86.67 mg L⁻¹, and temperature 293.4 K; the maximum NR removal rate was closely agreed with the theoretical predicted values of 96.6% which was suggested by Design Expert.

3.5. Adsorption kinetics

Adsorption kinetics models were used to explain the adsorption mechanism and characteristics. The most popular kinetic models [34], pseudo-first-order equation, and pseudo-second-order equation were

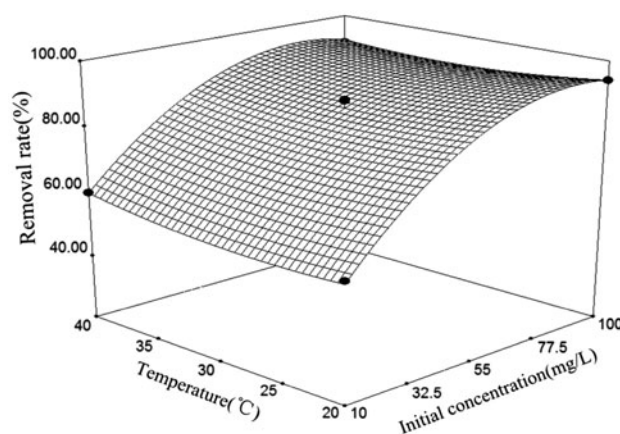


Fig. 6. The effects of temperature and initial concentration on NR removal.

employed in parallel to estimate possible reaction mechanisms and adsorption rates.

The pseudo-first-order equation could be expressed as the following Eq. (6):

$$\log(Q_e - Q_t) = \log Q_e - \frac{k_1}{2.303} t \quad (6)$$

where Q_e and Q_t (mg g⁻¹) were the amounts of NR adsorbed per unit weight of biosorbent at equilibrium and at time t , respectively; and k_1 (min⁻¹) was the constant rate of pseudo-first-order adsorption.

The parameters $Q_{e,cal}$ and k_1 could be obtained from the slope and intercept of plots ($\log(Q_e - Q_t)$ versus time). The Table 5 shows the parameters of pseudo-first-order equation. The values of the correlation coefficient r^2 were between 0.8513 and 0.962 at different NR concentrations. Moreover, the calculated $Q_{e,cal}$ (mg g⁻¹) were not correspond to $Q_{e,exp}$ (mg g⁻¹). This obviously indicated that the pseudo-first-order kinetic model was not appropriate to describe the adsorption. The results were similar to the NR adsorption by spent cottonseed hull substrate [18].

The pseudo-second-order equation based on adsorption equilibrium capacity could be expressed in liner form as Eq. (7) [16]:

$$\frac{t}{Q_t} = \frac{1}{k_2 Q_e^2} + \frac{1}{Q_e} t \quad (7)$$

where the k_2 (g mg⁻¹ min⁻¹) was constant rate of pseudo-second-order adsorption. The $Q_{e,cal}$ and k_2 could be determined by the slope and intercept of plots (t/Q_t versus time); the pseudo-second-order is illustrated in Fig. 7. The parameters are also given in Table 5. The values of the correlation coefficient r^2 from 0.997 to 1, which demonstrated that the adsorption data fitted the pseudo-second-order model well. And the calculated values of Q_e obtained from pseudo-second-order model agreed perfectly with the value of equilibrium adsorption quantity from the experiment; therefore, the pseudo-second-order model could predict the kinetic process in NR adsorption by PONS. The similar results were found by halloysite nanotubes [16], spent cottonseed hull substrate, [18] and peanut husk [35].

3.6. Adsorption isotherms

In this study, two common isotherm models, Langmuir and Freundlich model were employed to explore the adsorption mechanism.

Table 5
The parameters of kinetic for NR adsorption

Kinetic models	Dye concentration (mg L ⁻¹)			
	50	100	150	200
Pseudo-first-order				
$Q_{e,exp}$ (mg g ⁻¹)	15.4	31.45	46.22	61.06
$Q_{e,cal}$ (mg g ⁻¹)	4.21	2.516	6.433	8.059
k_1 (min ⁻¹)	0.0095	0.0188	0.0129	0.0144
r^2	0.8513	0.9505	0.962	0.9591
Pseudo-second-order				
$Q_{e,cal}$ (mg g ⁻¹)	15.15	31.446	46.296	61.728
k_2 (g mg ⁻¹ min ⁻¹)	0.014	0.0409	0.0061	0.0032
r^2	0.997	1	0.9996	0.9995

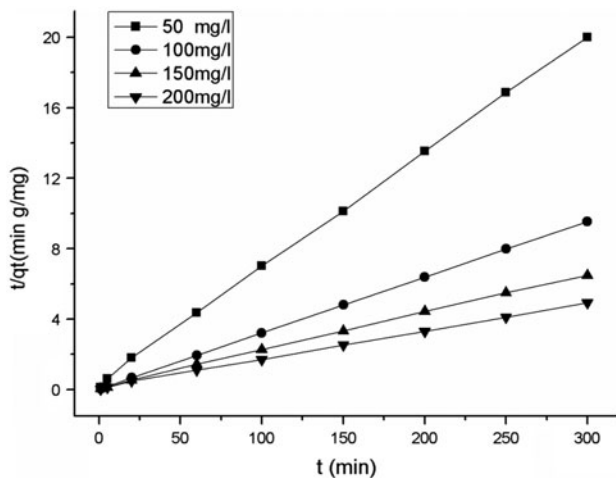


Fig. 7. Pseudo-second-order kinetic plots for NR adsorption onto PONS at 293 K.

The Langmuir adsorption isotherm was considered to be monolayer adsorption based on the molecular adsorption [11,36]. The linear form of Langmuir model was expressed as Eq. (8):

$$\frac{C_e}{Q_e} = \frac{1}{Q_m K_L} + \frac{C_e}{Q_e} \quad (8)$$

where C_e (mg L⁻¹) was the equilibrium concentration of NR in the solution; Q_e (mg g⁻¹) was the equilibrium concentration of NR on the PONS; Q_m (mg g⁻¹) was the maximum monolayer adsorption capacity; and K_L (L mg⁻¹) was the Langmuir model constant related to the heat of adsorption. The values of Q_m and K_L could be calculated by plotting C_e/Q_e vs. C_e . To confirm whether the adsorption was favorable, the dimensionless constant separation factor R_L was used and defined as the Eq. (9):

$$R_L = \frac{1}{1 + K_L C_0} \quad (9)$$

where K_L (L mg⁻¹) was the Langmuir model constant, and C_0 (mg L⁻¹) was the initial NR concentration. The value of R_L suggested the adsorption to be irreversible ($R_L = 0$), favorable ($0 < R_L < 1$), linear ($R_L = 1$), and unfavorable ($R_L > 1$) [37].

The Langmuir model parameters and R_L are shown in Table 6. The correlation coefficients (r^2) of the Langmuir equation were above 0.998 at three temperatures, so the adsorption was fitted to Langmuir isotherm very well. The values of R_L at three different temperatures were all between 0.0017 and 0.3135. Therefore, the three adsorption processes were favorable. And the maximum monolayer adsorption capacities of PONS were 57.14 mg g⁻¹ at 293 K, 59.17 mg g⁻¹ at 303 K, and 61.73 mg g⁻¹ at 313 K. The results illustrated that the NR covered the homogeneous surface of PONS.

The Freundlich isotherm model assumed that the adsorption took place on heterogeneous surfaces meanwhile with the interaction between the adsorbed molecules [38]. The linear form of Freundlich isotherm model was expressed as:

$$\ln Q_e = \ln K_F + \frac{1}{n} \ln C_e \quad (10)$$

where Q_e and C_e were defined as above, K_F (mg g⁻¹(mg L⁻¹)^{1/n}) were Freundlich constants related to adsorption capacity, higher value for K_F indicated higher affinity for adsorbate; the value of $1/n$ lied between 0.1 and 1 indicated a favorable adsorption process [39,40]. The r^2 , K_F , and $1/n$ were calculated and are shown in Table 6. The value of $1/n$ lied in a

Table 6
Isotherm model constants for NR adsorption

Isotherm models	Temperature (K)		
	293	303	313
Langmuir			
$Q_{max}(\text{mg g}^{-1})$	57.14	59.17	61.73
$K_L(\text{L mg}^{-1})$	0.293	0.266	0.219
R_L	0.0017–0.2544	0.0019–0.2732	0.0023–0.3135
r^2	0.9995	0.9992	0.9989
Freundlich			
$K_F(\text{mg g}^{-1}(\text{mg L}^{-1})^{1/n})$	34.678	35.311	37.055
$1/n$	0.0985	0.1011	0.0979
r^2	0.8498	0.8568	0.8685

favorable scope. The correlation coefficients (r^2) of Freundlich isotherm model were 0.8498 at 293 K, 0.8568 at 303 K, and 0.8685 at 313 K. The correlation coefficients (r^2) of Freundlich isotherm were smaller than the Langmuir equation, so the adsorption was fitted to the Langmuir model.

3.7. Adsorption thermodynamics

Thermodynamic parameter related to the adsorption process, free energy change (ΔG , kJ mol^{-1}) at 293, 303, and 313 K for adsorption were calculated using the Eq. (11) [41]:

$$\Delta G = -RT \ln K_L \quad (11)$$

where R is the universal gas constant ($8.314 \text{ J mol}^{-1} \text{ K}^{-1}$); T is the temperature (K), and K_L is Langmuir constant (L mol^{-1}) obtained from the plot of C_e/Q_e vs. C_e . The values of ΔG were $-27.64 \text{ kJ mol}^{-1}$ at 293 K, $-28.33 \text{ kJ mol}^{-1}$ at 303 K, and $-28.76 \text{ kJ mol}^{-1}$ at 313 K. The values of ΔG were negative, indicating the spontaneity and feasibility of these processes. What is more, the value of ΔG was decreased with increasing temperature, which revealed that adsorption was favorable at a higher temperature.

4. Conclusions

In the present study, PONS were demonstrated that it was feasible to remove NR from aqueous solution. The conclusions drawn were as follows:

- (1) SEM showed that the rough surface and the nanosize of PONS. The FTIR spectroscopy

directly demonstrated that the responsible functional groups such as $-\text{NH}$, $-\text{OH}$, $\text{C}=\text{O}$, $\text{P}=\text{O}$, $\text{P}-\text{OH}$, and $\text{C}=\text{N}=\text{C}$ participated in the adsorption process.

- (2) Min Run Res V design studied the six variables. The pH, initial concentration, and temperature were the main factors. Furthermore, the three significant factors further studied by BBD; the maximum removal rate 96.14% was obtained in optimal conditions, pH 3.56, initial NR concentration = 86.67 mg L^{-1} , and temperature 293.4 K.
- (3) The kinetic study at different initial concentrations indicated that the adsorption was better fitted to the pseudo-second-order model than the pseudo-first-order model. The adsorption equilibrium followed the Langmuir model, which gave the maximum adsorption capacity of 61.73 mg g^{-1} at 313 K. And the adsorption thermodynamics indicated the processes were spontaneous.

Acknowledgments

This study was financially supported by the Science and Technology Supportive Project of Sichuan Province, China (No. 2013SZ0062), Science and Technology Supportive Project of Chengdu (No. 12DXYB087JH-005) and NSFC (No. J1103518). The authors wish to thank Professor Guanglei Cheng and Dong Yu from Sichuan University for their technical assistance.

References

- [1] K.C. Chen, J.Y. Wu, D.J. Liou, S.C.J. Hwang, Decolorization of the textile dyes by newly isolated bacterial strains, *J. Biotechnol.* 101 (2003) 57–68.

- [2] T. Robinson, G. McMullan, R. Marchant, P. Nigam, Remediation of dyes in textile effluent: A critical review on current treatment technologies with a proposed alternative, *Bioresour. Technol.* 77 (2001) 247–255.
- [3] X. Dong, W. Ding, X. Zhang, X. Liang, Mechanism and kinetics model of degradation of synthetic dyes by UV-vis/H₂O₂/ferrioxalate complexes, *Dyes Pigm.* 74 (2007) 470–476.
- [4] R. Gong, Y. Ding, M. Li, C. Yang, H. Liu, Y. Sun, Utilization of powdered peanut hull as biosorbent for removal of anionic dyes from aqueous solution, *Dyes Pigm.* 64 (2005) 187–192.
- [5] L. Lu, M. Zhao, S.C. Liang, L.Y. Zhao, D.B. Li, B.B. Zhang, Production and synthetic dyes decolorization capacity of a recombinant laccase from *Pichia pastoris*, *J. Appl. Microbiol.* 107 (2009) 1149–1156.
- [6] M.A.M. Salleh, D.K. Mahmoud, W.A.W.A. Karim, A. Idris, Cationic and anionic dye adsorption by agricultural solid wastes: A comprehensive review, *Desalination* 280 (2011) 1–13.
- [7] E. Bulut, M. Özacar, İ.A. Şengil, Equilibrium and kinetic data and process design for adsorption of Congo Red onto bentonite, *J. Hazard. Mater.* 154 (2008) 613–622.
- [8] E. Lorenc-Grabowska, G. Gryglewicz, Adsorption characteristics of Congo Red on coal-based mesoporous activated carbon, *Dyes Pigm.* 74 (2007) 34–40.
- [9] X. Tian, C. Li, H. Yang, Z. Ye, H. Xu, Spent mushroom: A new low-cost adsorbent for removal of Congo Red from aqueous solutions, *Desalin. Water Treat.* 27 (2011) 319–326.
- [10] W. Zhang, H. Yang, L. Dong, H. Yan, H. Li, Z. Jiang, X. Kan, A. Li, R. Cheng, Efficient removal of both cationic and anionic dyes from aqueous solutions using a novel amphoteric straw-based adsorbent, *Carbohydr. Polym.* 90 (2012) 887–893.
- [11] L.-C. Juang, C.-C. Wang, C.-K. Lee, Adsorption of basic dyes onto MCM-41, *Chemosphere* 64 (2006) 1920–1928.
- [12] A.E. Ofomaja, Equilibrium sorption of methylene blue using mansonia wood sawdust as biosorbent, *Desalin. Water Treat.* 3 (2009) 1–10.
- [13] H. Metivier-Pignon, C. Faur, P.L. Cloirec, Adsorption of dyes onto activated carbon cloth: Using QSPRs as tools to approach adsorption mechanisms, *Chemosphere* 66 (2007) 887–893.
- [14] P. Sudamalla, S. Pichiah, M. Manickam, Responses of surface modeling and optimization of Brilliant Green adsorption by adsorbent prepared from *Citrus limetta* peel, *Desalin. Water Treat.* 50 (2012) 367–375.
- [15] V. Gupta, Application of low-cost adsorbents for dye removal—A review, *J. Environ. Manage.* 90 (2009) 2313–2342.
- [16] P. Luo, Y. Zhao, B. Zhang, J. Liu, Y. Yang, Study on the adsorption of Neutral Red from aqueous solution onto halloysite nanotubes, *Water Res.* 44 (2010) 1489–1497.
- [17] L. Liu, Y. Wan, Y. Xie, R. Zhai, B. Zhang, J. Liu, The removal of dye from aqueous solution using alginate-halloysite nanotube beads, *Chem. Eng. J.* 187 (2012) 210–216.
- [18] Q. Zhou, W. Gong, C. Xie, D. Yang, X. Ling, X. Yuan, S. Chen, X. Liu, Removal of Neutral Red from aqueous solution by adsorption on spent cottonseed hull substrate, *J. Hazard. Mater.* 185 (2011) 502–506.
- [19] P. Kaushik, A. Malik, Fungal dye decolorization: Recent advances and future potential, *Environ. Int.* 35 (2009) 127–141.
- [20] A. Srinivasan, T. Viraraghavan, Decolorization of dye wastewaters by biosorbents: A review, *J. Environ. Manage.* 91 (2010) 1915–1929.
- [21] S. Di Gregorio, F. Balestri, M. Basile, V. Matteini, F. Gini, S. Giansanti, M.G. Tozzi, R. Basosi, R. Lorenzi, Sustainable discoloration of textile chromo-baths by spent mushroom substrate from the industrial cultivation of *Pleurotus ostreatus*, *J. Environ. Prot.* 1 (2010) 85–94.
- [22] X. Jing, Y. Cao, X. Zhang, D. Wang, X. Wu, H. Xu, Biosorption of Cr (VI) from simulated wastewater using a cationic surfactant modified spent mushroom, *Desalination* 269 (2011) 120–127.
- [23] X. Song, H. Liu, L. Cheng, Y. Qu, Surface modification of coconut-based activated carbon by liquid-phase oxidation and its effects on lead ion adsorption, *Desalination* 255 (2010) 78–83.
- [24] Y. Cao, Z. Liu, G. Cheng, X. Jing, H. Xu, Exploring single and multi-metal biosorption by immobilized spent *Tricholoma lobayense* using multi-step response surface methodology, *Chem. Eng. J.* 164 (2010) 183–195.
- [25] S.S. Moghaddam, M.R. Alavi Moghaddam, M. Arami, Response surface optimization of Acid Red 119 dye adsorption by mixtures of dried sewage sludge and sewage sludge ash, *CLEAN–Soil Air Water* 40 (2012) 652–660.
- [26] M. Li, C. Feng, Z. Zhang, R. Chen, Q. Xue, C. Gao, N. Sugiura, Optimization of process parameters for electrochemical nitrate removal using Box–Behnken design, *Electrochim. Acta.* 56 (2010) 265–270.
- [27] E. Hamed, A. Sakr, Application of multiple response optimization technique to extended release formulations design, *J. Controlled Release* 73 (2001) 329–338.
- [28] M. Rajkumar, H. Freitas, Influence of metal resistant-plant growth-promoting bacteria on the growth of *Ricinus communis* in soil contaminated with heavy metals, *Chemosphere* 71 (2008) 834–842.
- [29] S.T. Akar, A. Gorgulu, Z. Kaynak, B. Anilan, T. Akar, Biosorption of Reactive Blue 49 dye under batch and continuous mode using a mixed biosorbent of macrofungus *Agaricus bisporus* and *Thuja orientalis* cones, *Chem. Eng. J.* 148 (2009) 26–34.
- [30] Z. Zhang, H. Zheng, Optimization for decolorization of azo dye acid green 20 by ultrasound and H₂O₂ using response surface methodology, *J. Hazard. Mater.* 172 (2009) 1388–1393.
- [31] B. Kayan, B. Gözmen, Degradation of Acid Red 274 using H₂O₂ in subcritical water: Application of response surface methodology (RSM), *J. Hazard. Mater.* 201–202 (2011) 100–106.
- [32] K.P. Singh, A.K. Singh, S. Gupta, S. Sinha, Optimization of Cr (VI) reduction by zero-valent bimetallic nanoparticles using the response surface modeling approach, *Desalination* 270 (2011) 275–284.
- [33] P. Tripathi, V.C. Srivastava, A. Kumar, Optimization of an azo dye batch adsorption parameters using Box–Behnken design, *Desalination* 249 (2009) 1273–1279.
- [34] W. Plazinski, W. Rudzinski, A. Plazinska, Theoretical models of sorption kinetics including a surface

- reaction mechanism: A review, *Adv. Colloid Interface Sci.* 152 (2009) 2–13.
- [35] R. Han, P. Han, Z. Cai, Z. Zhao, M. Tang, Kinetics and isotherms of Neutral Red adsorption on peanut husk, *J. Environ. Sci.* 20 (2008) 1035–1041.
- [36] F. Ge, H. Ye, M.M. Li, B.X. Zhao, Efficient removal of cationic dyes from aqueous solution by polymer-modified magnetic nanoparticles, *Chem. Eng. J.* 198–199 (2012) 11–17.
- [37] M. Arami, N.Y. Limaee, N.M. Mahmoodi, Investigation on the adsorption capability of egg shell membrane towards model textile dyes, *Chemosphere* 65 (2006) 1999–2008.
- [38] Y. Liu, Q. Zhao, G. Cheng, H. Xu, Exploring the mechanism of lead (II) adsorption from aqueous solution on ammonium citrate modified spent *Lentinus edodes*, *Chem. Eng. J.* 173 (2011) 792–800.
- [39] V.K. Gupta, C. Jain, I. Ali, S. Chandra, S. Agarwal, Removal of lindane and malathion from wastewater using bagasse fly ash—A sugar industry waste, *Water Res.* 36 (2002) 2483–2490.
- [40] A. Safa Özcan, B. Erdem, A. Özcan, Adsorption of Acid Blue 193 from aqueous solutions onto Na-bentonite and DTMA-bentonite, *J. Colloid Interface Sci.* 280 (2004) 44–54.
- [41] E. Salehi, S. Madaeni, F. Heidary, Dynamic adsorption of Ni(II) and Cd(II) ions from water using 8-hydroxyquinoline ligand immobilized PVDF membrane: Isotherms, thermodynamics and kinetics, *Sep. Purif. Technol.* 94 (2012) 1–8.